IOPscience iopscience.iop.org

Home Search Collections Journals About Contact us My IOPscience

Analysis of local electrical properties of grain boundaries in Si by electron-beam-induced-current techniques

This article has been downloaded from IOPscience. Please scroll down to see the full text article.

2002 J. Phys.: Condens. Matter 14 13161

(http://iopscience.iop.org/0953-8984/14/48/364)

View the table of contents for this issue, or go to the journal homepage for more

Download details:
IP Address: 171.66.16.97
The article was downloaded on 18/05/2010 at 19:16

Please note that terms and conditions apply.

INSTITUTE OF PHYSICS PUBLISHING JOURNAL OF PHYSICS: CONDENSED MATTER

J. Phys.: Condens. Matter **14** (2002) 13161–13168 PII: S0953-8984(02)54030-3

Analysis of local electrical properties of grain boundaries in Si by electron-beam-induced-current techniques

S Pandelov[1,3], **W Seifert**[1,2], **M Kittler**[1,2] **and J Reif**[1,3]

[1] Joint Lab IHP/BTU, Universitätsplatz 3-4, 03044 Cottbus, Germany
[2] IHP, Im Technologiepark 25, 15236 Frankfurt (Oder), Germany
[3] BTU Cottbus, LS Experimentalphysik II, Universitätsplatz 3-4, 03044 Cottbus, Germany

Received 27 September 2002
Published 22 November 2002
Online at stacks.iop.org/JPhysCM/14/13161

Abstract
We report on temperature-dependent investigations of grain boundaries (GB) in p-type multicrystalline Si by means of two different electron-beam-induced-current (EBIC) methods. The so-called GB-EBIC technique is used to estimate the barrier height of the GB as a function of beam current and temperature. The barrier is found to decrease upon increase of injection level and decrease of temperature. EBIC investigations in standard geometry were performed for comparison. It is shown that the two EBIC techniques yield different information about the GB. Possible reasons of this behaviour are discussed.

1. Introduction

The recombination activity of extended defects such as dislocations and grain boundaries (GB) in Si has been attracting much attention over recent decades because of both its technological importance and its still incompletely understood physics. Currently, increased interest in this issue has been triggered by the fast development of Si photovoltaics. The use of low-cost multicrystalline Si for solar cells demands alternative strategies for defect engineering since crystal defects/dislocations are inherent in this material. Hence, improved knowledge about the relationship between the electrical properties of defects, their structure and interaction with impurities is essential.

Considerable progress has recently been made in understanding the behaviour of dislocations. The recombination strength of dislocations was found to be controlled by the amount of impurities in/near their core [1]. Moreover, it was demonstrated that the temperature behaviour of the recombination activity of dislocations measured with the electron-beam-induced-current (EBIC) technique gives quantitative access to the amount of contamination at dislocations [2].

Compared to that at dislocations, recombination at GBs has only limited impact on the efficiency of recently developed large-grained multicrystalline cells. Nevertheless, it is

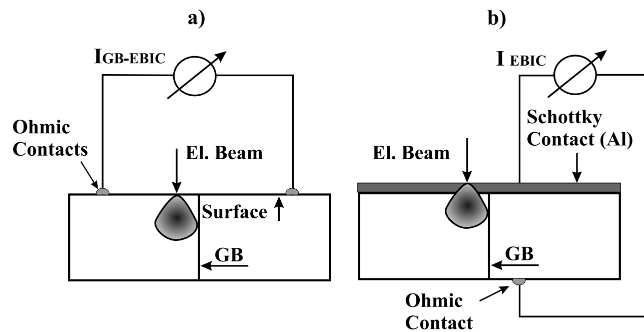

Figure 1. Set-ups appropriate for GB characterization: (a) GB-EBIC, (b) standard EBIC.

believed that studying the electrical activity of GBs still may substantially contribute to solving the efficiency problem, specifically by improving our understanding of the basic mechanisms of interaction between defects and impurities. EBIC in standard geometry, with a p–n or Schottky junction perpendicular to the GB, is usually used for local GB characterization [3–5]. Palm [6] carried out GB studies with a different geometry, first proposed by Mataré and Laaksoo [7] and referred to as GB-EBIC here. He showed that this geometry allows a local determination of both GB barrier height and recombination parameters, and hence represents a promising approach for tackling the issue of GB electrical activity. Unfortunately, this approach has not been applied to systematic studies since then. Also, to our knowledge, the technique was used only at room temperature, although variation of the temperature can yield a more detailed insight into defect (e.g. dislocation [1, 2]) properties.

In this paper we will report on temperature-dependent EBIC investigations of GBs in mc-Si. GB-EBIC was used to estimate the height of the GB potential barrier as a function of temperature and injection level/beam current. EBIC investigations in standard geometry were carried out to provide complementary information on GB activity.

2. Experimental details

Boron-doped p-type (2×10^{16} cm^{-3}) cast multicrystalline silicon was used in the investigation. To remove damage, the samples were etched in HNO_3/HF/CH_3COOH until a shiny surface was obtained. Ohmic contacts were prepared by rubbing In/Ga onto the surface. Schottky contacts were prepared by Al evaporation.

The sample is placed in a scanning electron microscope (Cambridge Stereoscan S360) equipped with a liquid nitrogen cold stage. The current signal from the amplifier (Matelect Induced Signal Monitor) can be displayed directly on the screen or digitized, stored and evaluated in a computer. Measurements were typically performed at a beam energy of 30 keV. The beam current I_b was varied in the range between about 20 pA and 20 nA. For GB-EBIC, the GB region of interest received a prolonged electron beam irradiation at high beam current and low beam energy prior to measurements. This procedure ensured high, but stable recombination velocity at the sample surface [8] which is important for obtaining reliable data. The sample temperature was varied between 300 and 80 K.

Figure 1 shows the two set-ups used for GB characterization. In the case of GB-EBIC, two small ohmic contacts are placed in the grains on both sides of the boundary of interest. The current through the connected amplifier is driven by the electric field of the GB barrier. An Al Schottky contact on the front surface and an ohmic contact on the rear are used in the

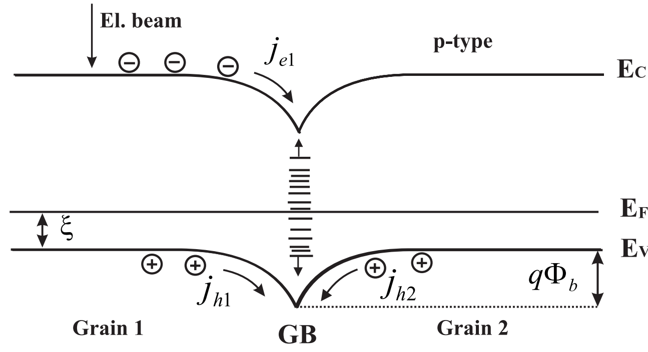

Figure 2. An illustration of the band scheme and currents at the GB under conditions of GB-EBIC (p-type Si): j_{e1}: current of beam-generated electrons (minority carriers); j_{h1}, j_{h2}: hole (majority carrier) currents from both grains towards the GB.

standard EBIC method, with the field of the Schottky junction driving the current. GB-EBIC investigations were performed first. Then, the In/Ga contacts on the front side were removed and the surface slightly etched before preparing the Al contact for standard EBIC investigation.

Measurements of the GB conductance as described in [6] were performed in GB-EBIC geometry both in the dark and with electron beam excitation, applying small bias voltages up to 3 mV to the Ohmic contacts. Special attention was paid to correctly accounting for the different resistances in the equivalent circuit of the GB-EBIC set-up (GB resistance, bulk resistance, contact resistance).

3. Basic information on GB behaviour

The situation at a GB under conditions of GB-EBIC is illustrated in figure 2. The GB can be described by a double-depletion-layer model. The minority carriers generated by the electron beam diffuse to the GB, are attracted by the electric field and recombine with holes in localized states at the boundary. The states are refilled with holes from both sides of the GB which overcome the barrier by thermal excitation. This results in a recombination current whose size depends on the number of carriers generated. For details of the processes, we refer the reader to [6]. The net current detected with the amplifier is

$$I_{GB-EBIC} = I_{e1} - I_{h1} = I_{h2} \tag{1a}$$

and since $I_{h1} = I_{h2}$ for low injection,

$$I_{GB-EBIC} = 0.5 I_{e1}. \tag{1b}$$

The current density of holes captured at the boundary can be described by an expression from thermionic emission theory [9]:

$$j_{h1,2} = cA \exp[-(\Phi_b + \xi)/kT], \tag{2}$$

with A the pseudo-Richardson constant ($A = A^*T^2$, $A^* = 120 \times 0.66$ A cm^{-2} K^{-2} for p-type Si [9]), Φ_b the barrier height, ξ the position of the Fermi level in the bulk and c the fraction of holes captured by the GB states. c is related to the number of states and their capture cross-section and was shown to be much smaller than unity [6].

The resistance of the GB, R_d, at equilibrium (in the 'dark') and small bias voltages ($qU \ll kT$) is given by

$$R_d = \left[\frac{qF_d}{kT} A \exp[-(\Phi_d + \xi)/kT]\right]^{-1}. \tag{3a}$$

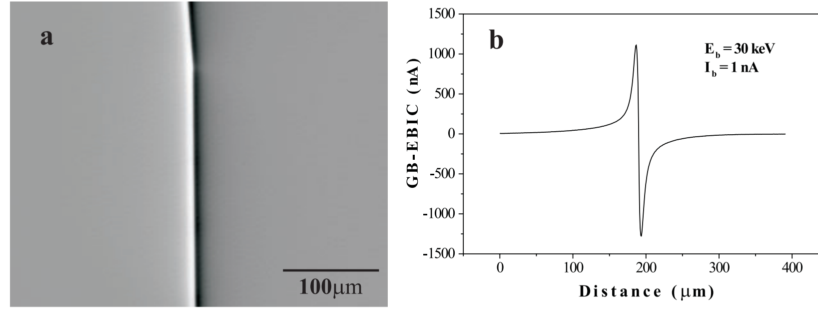

Figure 3. GB image (a) and current profile (b) obtained with the GB-EBIC set-up.

with Φ_d the equilibrium (dark) height of the barrier and F_d the total area of the boundary. Excitation by a focused electron beam reduces the barrier locally, resulting in a corresponding decrease of the GB resistance. The GB resistance can be represented by two parallel resistances: the dark resistance, R_d, and the resistance of a small area excited by the beam, R_b. With the electron beam positioned at the GB, this area is defined by the diameter of the generation volume [6]. The following equation holds:

$$R_b = \left[\frac{qF_b}{kT}A\exp[-(\Phi_b + \xi)/kT]\right]^{-1} \tag{3b}$$

where Φ_b is the barrier under excitation and $F_b = d^2$; d is the diameter of the generation volume.

Hence, we may estimate the local barrier height under excitation from measurements of R_b using the relation

$$\Phi_b = -kT\ln\left[\frac{kT}{qAR_bF_b}\right] - \xi. \tag{4}$$

Please note that all resistances in the current path (bulk, contacts, internal resistance of amplifier) should be taken into account to get meaningful results.

4. Results

Figure 3 shows a typical GB-EBIC image and the corresponding current profile. It is important to note that not all GBs yield considerable GB-EBIC signals. Some GBs did not show a GB-EBIC signal, despite a high recombination activity detected with the standard EBIC method. The characteristic bright/dark contrast reflects the different directions of the electric field in the potential barrier of the boundary. Maximum signal is obtained when the edge of the generation volume touches the GB. The decay of the signal on both sides of the boundary is diffusion induced and allows one to estimate the diffusion length in both grains adjacent to the boundary. The slight asymmetry visible in the profile may be caused by differences in diffusion length or surface recombination velocity of the two grains. An asymmetry may also be caused by a non-perpendicular GB. The GB-EBIC signal represents a recombination current characterizing the recombination activity of the GB. Figure 4 depicts its dependence on beam current and temperature. The GB-EBIC signal shows an approximately linear dependence on beam current at low injection. Up to 30% of the minority carriers generated are collected by the GB barrier in this range. As expected, the slope of the curves decreases with increasing injection level due to a constant decrease of the recombination velocity in the GB plane. For

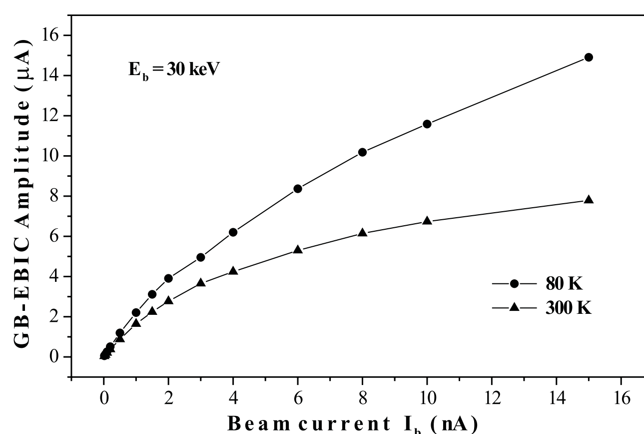

Figure 4. Amplitude of the GB signal versus beam current at 300 and 80 K.

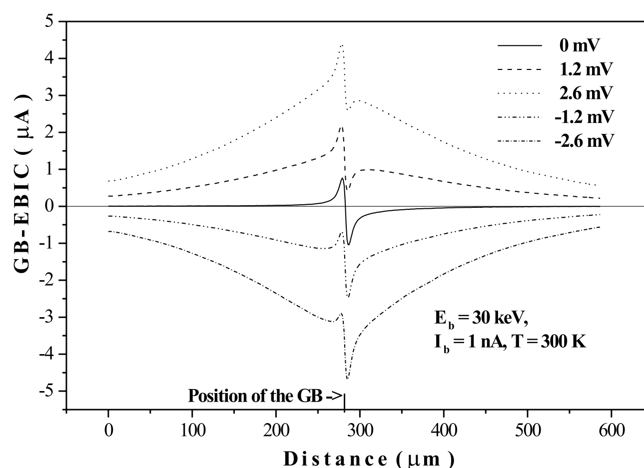

Figure 5. GB-EBIC profiles as a function of the bias voltage applied to the Ohmic contacts.

$I_b = 15$ nA the fraction of collected minority carriers is only 6% at 300 and 13% at 80 K. This points to a higher recombination activity of the GB at low temperatures. Such behaviour is often observed at GBs and dislocations, but was not confirmed by temperature-dependent measurements of this GB using the standard EBIC method.

Results of the measurements under small bias voltage are presented in figure 5. The curves show the change of the current through the amplifier when the electron beam is moved across the boundary. The constant dark current that is caused by the applied bias has already been subtracted. It is found that the measured signals scale with the applied voltage. The signal recorded at $U = 0$ mV is just the normal GB-EBIC signal. The curves can easily be analysed bearing in mind that they consist of two constituents (see the schematic illustration in figure 6). The first current component is due to a decrease of the GB resistance (figure 6(a)). This is the component that we are mainly interested in for estimating the barrier height. Its origin can be explained as follows. When the electron beam is far away, a current, as under dark conditions, is observed. With decreasing distance between the electron probe and boundary, more and more minority carriers reach the boundary and cause a local decrease of the barrier height and

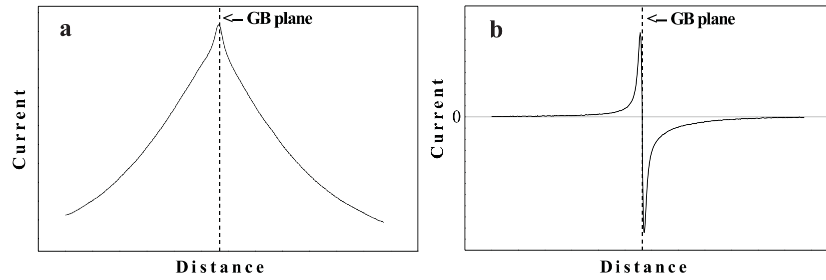

Figure 6. A schematic illustration of current components contributing to the profiles observed under an applied bias (see figure 5). (a) The current due to the beam-induced decrease of the GB resistance. (b) The recombination current related to the presence of an electric field and recombination levels.

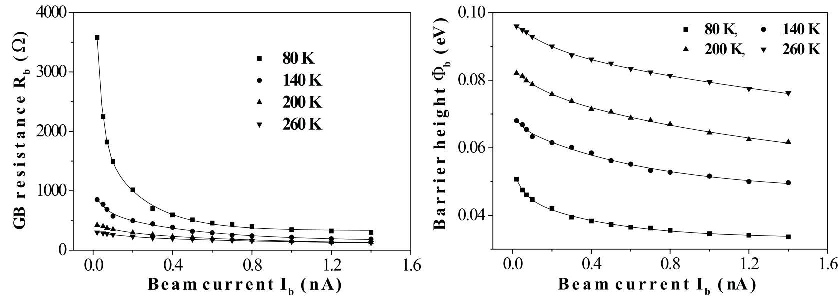

Figure 7. Dependences of GB properties on beam current for different temperatures between 80 and 260 K: GB resistance when the electron beam is positioned at the GB and the barrier height deduced from R_b using relation (4).

a corresponding decrease of resistance. This leads to an increase of the bias-driven current, which will be at its maximum when the beam is positioned at the GB. From the maximum of this current component we obtain the resistance of the small part of the GB that is influenced by the electron beam. The second current component (figure 6(b)) is the recombination current induced by the field of the boundary. Hence, to obtain the resistance component we have to subtract the current profile obtained without bias from profiles obtained under a bias voltage. This procedure was applied to measurements at different temperatures and beam currents. The results are represented in figure 7. Figure 7(a) shows the GB resistance data and figure 7(b) the barrier height calculated from those data using relation (4). We found a decrease of the barrier height with decreasing temperature and increasing beam current. The latter is an expected result, although the low values compared to the case of the dark barrier (table 1) may be surprising at first glance. The temperature dependence obtained was not expected. The same type of temperature dependence was, however, also found for the barrier height in the dark (table 1).

Investigations of the GB in standard EBIC geometry were performed with the aim of obtaining complementary information about its properties. Figure 8 shows an EBIC image obtained under these different conditions. The imaged area corresponds to that in figure 3. The GB exhibits a rather moderate recombination activity, except at a few isolated spots. The EBIC contrast amounts to about 5% in the region of homogeneous activity, i.e. about 5% of the minority carriers generated recombine at the boundary. In the dark spots the recombination activity is higher by a factor of up to about 3. The observed inhomogeneity

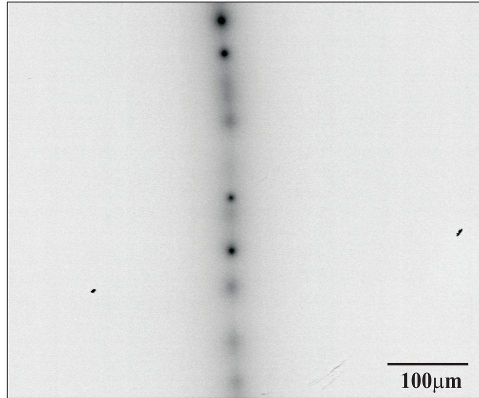

Figure 8. The same GB as in figure 3, but imaged with standard EBIC ($E_b = 30$ keV, $T = 300$ K). Note the rather moderate contrast of the boundary and the dark spots along it.

Table 1. GB resistance R_d and barrier height Φ_d at equilibrium (in the 'dark').

Temperature (K)	R_d (Ω)	Φ_b (eV)
80	281	0.103
140	154	0.170
200	110	0.233
260	81	0.300
290	65	0.320

of the GB recombination activity is in contradiction to the results obtained with GB-EBIC (figure 3). Moreover, the recombination activity seen in the standard EBIC approach did not change substantially upon cooling, while the GB-EBIC signal showed a clear increase at low temperatures. To conclude, no obvious correlation between the GB-EBIC and the standard EBIC was found.

5. Discussion and conclusions

We were able to determine GB barrier heights as a function of injection level and temperature from resistivity and GB-EBIC data. The injection level dependence indicates that the GB barrier is very sensitive to the level of excitation. While the dark barrier is about 300 mV at room temperature, its value under excitation does not exceed 100 mV even for the lowest beam currents used. The same sudden change in barrier height is observed for other temperatures. Unfortunately, the transition from dark barrier to barrier under low excitation could not be addressed in more detail, because measurements at beam currents below 20 pA could not be performed due to a poor signal-to-noise ratio.

The barrier was generally found to decrease with temperature. This is a result that cannot be explained with a homogeneous GB since GB charge (and consequently barrier height) should rather increase when the temperature decreases and the Fermi level moves toward the valence band edge. However, the observed decrease of the effective barrier height may be caused by inhomogeneities of the barrier height. According to Werner [10], the effective barrier height is always smaller than the average barrier if potential fluctuations exist at the boundary. The difference between effective barrier and average barrier increases with

decreasing temperature. It was also shown in [10] that even single grain boundaries in bicrystals were inhomogeneous. Accordingly, it is likely that barrier inhomogeneities are responsible for the temperature dependence of the effective GB barrier in the sample studied. Since the GB-EBIC approach did not reveal inhomogeneities, such spatial fluctuations should take place on a scale of not more than a few micrometres. Unfortunately, the data regarding the temperature dependence were not accurate enough for an analysis in terms of mean barrier and fluctuations. Because of this, we abandoned the idea of performing a detailed analysis as described in [6].

Another possible explanation of the temperature behaviour might be the existence of an additional conduction path, e.g. at the surface of the sample.

The GB-EBIC and standard EBIC methods provide different information about the GB. We found that GBs may show high activity with GB-EBIC geometry, but rather low activity with standard EBIC geometry. Vice versa, boundaries with strong recombination activity may not exhibit a GB-EBIC signal at all. This is because the GB-EBIC requires the presence of both barrier and recombination centres. A GB with a certain recombination activity that is not charged is therefore detected only with the standard EBIC method. An additional difference that may show up in studies involving both techniques is the state of the sample surface (surface recombination velocity, stability). Figures 3 and 8 show examples of another intriguing difference which is not understood so far: homogeneous versus dotted contrast.

Despite the difficulties encountered, we believe that the combination of the two EBIC techniques has the potential to shed more light on the behaviour of GBs. More investigations are however needed to solve open questions and to reach the final goal of a unified description of the GB behaviour based on combined application of the GB-EBIC and standard EBIC approaches.

References

[1] Kittler M, Ulhaq-Bouillet C and Higgs V 1995 *J. Appl. Phys.* **78** 4573
[2] Kveder V, Kittler M and Schröter W 2001 *Phys. Rev.* B **63** 115208
[3] Marfaing Y and Maurice J L 1991 *Polycrystalline Semiconductors* vol 2 (Berlin: Springer) p 205
[4] Marek J 1982 *J. Appl. Phys.* **53** 1454
[5] Donolato C 1983 *J. Appl. Phys.* **54** 1314
[6] Palm J 1993 *J. Appl. Phys.* **74** 1169
[7] Mataré H F and Laaksoo C W 1968 *Appl. Phys. Lett.* **13** 216
[8] Kittler M and Lärz J 1998 *Solid State Phenom.* **63–64** 77
[9] Sze S M 1981 *Physics of Semiconductor Devices* (New York: Wiley)
[10] Werner J H 1994 *Solid State Phenom.* **37–38** 213